

Reclamation and Additional Alloying of 18Ni(350) Maraging Steel

M. Ahmed, I. Salam, I. Nasim, S.W. Hussain, F.H. Hashmi, and A.Q. Khan

The possibility of gainfully utilizing grade 18Ni(350) maraging steel scrap has been investigated, along with the effect of additional alloying with niobium. A vacuum induction melting and casting furnace was used for melting and additional alloying. The cast ingots were hot forged and their properties compared with those of the stock material. The composition of the reprocessed material was found to be within the prescribed range for 18Ni(350) steel, except for some loss in titanium content. The hardness and tensile strength of the recycled steel were similar to those of the stock material. A slight decrease in hardness in the aged condition could be attributed to loss of titanium during remelting. Charpy V-notch impact testing indicated significantly higher toughness in the remelted material; this has been attributed to a homogeneous, refined microstructure and a lower level of inclusions. Additional alloying with 2% Nb not only improved the mechanical properties but also affected the amount of reverted austenite obtained after aging.

Keywords

additional alloying, charpy impact strength, electron microscopy, inclusions, maraging steel, reclamation, tensile strength, vacuum melting

1. Introduction

MARAGING steels possess exceptionally high hardness and toughness (Ref 1-3). In the annealed condition, a relatively soft martensite is obtained, which can be easily worked into many required shapes. Maximum hardness is obtained by aging in the temperature range between 480 and 510 °C (Ref 2). Aging causes precipitation of intermetallics, such as Ni₃Ti, Ni₃(TiMo), and Fe₂Mo (Ref 2,4). Aging beyond 550 °C causes softening due to formation of reverted austenite (Ref 5, 6). In applications where magnetic properties are of interest, aging normally is carried out at temperatures between 550 and 650 °C (Ref 7).

Conventionally, a two-stage melting practice is adopted to minimize segregation and inclusion levels in high-alloy steels such as maraging steel. Because maraging steels contain reactive elements (e.g., titanium), alloying is invariably carried out under vacuum. The ingots produced are subjected to secondary refining through remelting by either vacuum arc remelting (VAR) or electroslag refining (ESR). Both of these techniques reduce the level of macro- as well as microsegregation. When ESR is employed, the level of sulfur and other nonmetallic inclusions can also be reduced.

The processing techniques involved, and the expensive alloying elements used (e.g., cobalt), make maraging steel an expensive commodity. Reclamation of scrap can result in substantial savings (Ref 8). In the present work we have explored the possibility of gainfully utilizing maraging steel scrap by remelting in a vacuum induction furnace. The stock material was received in the form of hot extruded rods with a diameter of 200 mm. Before extrusion, the ingots were subjected

to ESR. Components rejected because of machining faults were used as charge for remelting in the furnace. The objective was to investigate whether intermediate refining could be avoided without compromising the properties of the material. Another important consideration was to note losses encountered during remelting and unwanted pickup due to metal/crucible and metal/mold interaction.

Additional alloying with niobium was carried out to determine the effect of this element on mechanical properties. The properties of the remelted and forged material were compared with those of the stock material.

2. Experimental Method

Maraging steel scrap of 18Ni(350) grade was remelted in a 14 kg capacity vacuum induction melting and casting furnace. The scrap was cleaned by sandblasting and subsequent vapor degreasing. Melting was carried out in a magnesium oxide crucible. The pressure during melting was on the order of 10⁻³ Pa. Ingots were prepared by pouring the melt into a graphite mold coated with a mixture of yttria and clay. The mold was designed to contain the shrinkage cavity in the top portion of the ingot, which was cut off before further processing. The cast ingots (100 mm in diameter) were then hot forged. The material was soaked at 1250 °C for 3 h; then a 40% reduction in cross section was achieved using a 500 kg pneumatic hammer. Next, the material was reheated at 1250 °C for 30 min. Another 40% reduction in cross section was carried out, followed by air cooling.

Tensile strength and Charpy V-notch impact energy values were determined using standard specimens as per ASTM specifications. The heat treatment was carried out in a vacuum furnace. Annealing and aging temperatures were fixed at 820 and 480 °C, respectively. These temperatures were found to be inappropriate for the case of additionally alloyed steels (see the next section). A Vickers hardness testing machine was used to determine the hardness of the material. Microstructural details were examined using scanning electron microscopy (SEM) and scanning transmission electron microscopy (STEM); specimens were electrolytically thinned using 20 vol% perchloric acid in ethanol at -30 °C.

M. Ahmed, I. Salam, I. Nasim, S.W. Hussain, F.H. Hashmi, and A.Q. Khan, Dr. A.Q. Khan Research Laboratories, P.O. Box 502, Rawalpindi, Pakistan

3. Results and Discussion

The chemical compositions of the stock and the remelted material are given in Table 1. It is evident that the composition of the remelted material was within the specification of maraging steel grade 350. However, titanium content was lower compared with the starting material. The average titanium loss was found to be on the order of 10%.

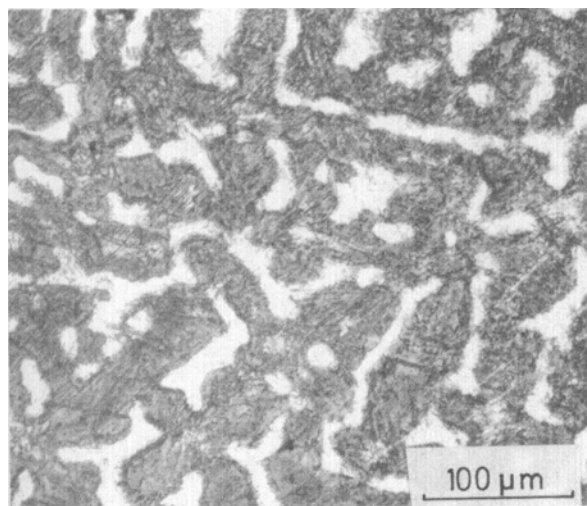
The as-cast structure of the reprocessed material is presented in Fig. 1(a). Energy-dispersive x-ray (EDX) analysis showed that the average titanium content in the dendrites was 2.2 wt%, compared to 1.35 wt% in the interdendritic zones. X-ray diffractograms obtained from the as-cast material showed that it consisted of martensite. A refined, homogeneous structure was obtained following hot forging (Fig. 1b).

The average grain size in the forged material was $15 \pm 5 \mu\text{m}$. In contrast, the average grain size of the stock material was in the range of $40 \pm 10 \mu\text{m}$. Grain size of the forged material was dependent on final forging temperature. In the present case, forging was continued until the temperature dropped to around 700°C .

The results of hardness, tensile strength, and Charpy V-notch impact tests for the reprocessed material in both the annealed and the aged conditions are presented in Table 2. Values obtained for the stock material are also given for comparison.

Table 1 Compositions of stock and reprocessed material

Element	Composition, wt%	
	Stock material	Reprocessed material
Nickel	18.1 ± 0.2	17.6 ± 0.4
Cobalt	12.6 ± 0.3	12.5 ± 0.3
Titanium	1.70 ± 0.10	1.50 ± 0.05
Molybdenum	3.7 ± 0.2	3.6 ± 0.4
Silicon	0.10	0.08
Aluminum	0.15	0.13
Carbon	0.005	<0.01
Sulfur	0.003	<0.01



(a)

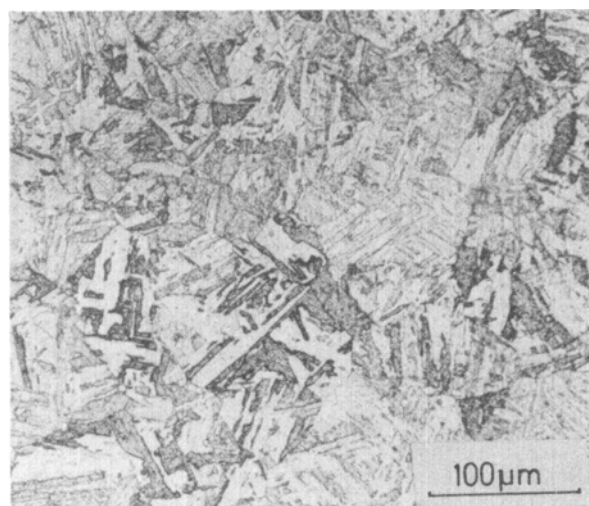
The hardness of the reprocessed material after aging at 480°C for 3 h was $660 \pm 5 \text{HV}$, compared to $700 \pm 5 \text{HV}$ for the stock material. As mentioned earlier, titanium loss occurs during re-melting. This reduces the amount of Ni_3Ti precipitates that form following aging. The reduction in hardness, therefore, is clearly related to the loss of titanium. However, the tensile strength of the reprocessed material in the aged condition was $2450 \pm 50 \text{MPa}$, slightly higher than the value of $2340 \pm 70 \text{MPa}$ obtained for the stock material.

A sharp difference in Charpy V-notch impact values was observed. In the annealed condition, these values for the reprocessed and the stock material were 120 ± 5 and $10 \pm 2 \text{J}$, respectively. The corresponding values after aging at 480°C for 3 h were 16 ± 3 and $4 \pm 1 \text{J}$, respectively. This difference in fracture toughness is also reflected in the fractographs of these materials shown in Fig. 2. In the low-magnification image (Fig. 2a), a mixed mode of fracture is evident in the stock material; that is, both intergranular and transgranular modes are present. The region where fracture occurred predominantly by the transgranular mode is shown in the higher-magnification image (Fig. 2b). The morphology exhibited appears to be due to remanence of the cast structure. The reduction ratio achieved during the extrusion process was not mentioned by the supplier; however, it appears that even after ESR, hot working was

Table 2 Results of hardness, tensile, and impact testing

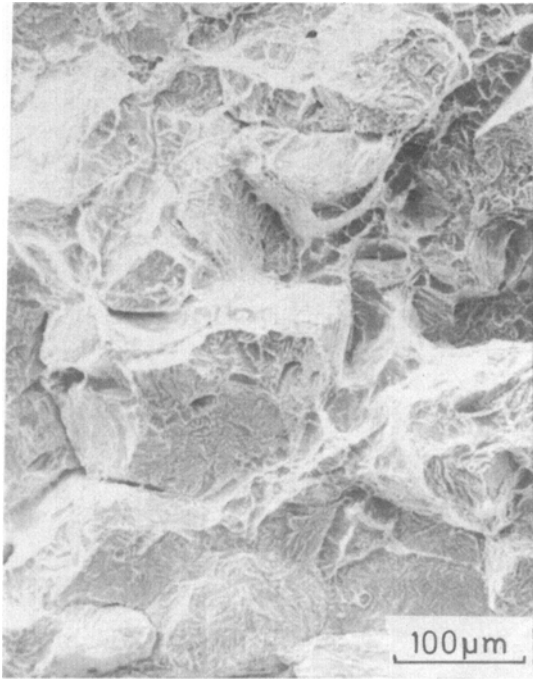
Test	Sample condition(a)	Stock material	Reprocessed material
Average grain size, μm	As forged	40 ± 10	15 ± 5
Hardness, HV	Annealed	350 ± 5	350 ± 5
	Aged	700 ± 10	660 ± 5
Tensile strength, MPa	Annealed	1180 ± 35	1173 ± 30
	Aged	2346 ± 70	2450 ± 50
Charpy V-notch impact values, J	Annealed	10 ± 2	120 ± 10
	Aged	4 ± 1	16 ± 3

(a) Annealed at 820°C for 30 min; aged at 480°C for 3 h



(b)

Fig. 1 Optical micrographs depicting (a) as-cast and (b) as-forged microstructures



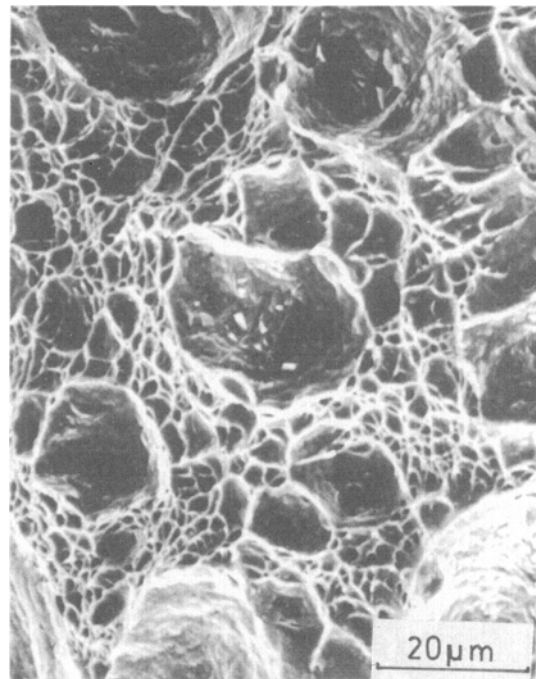
(a)



(b)



(c)



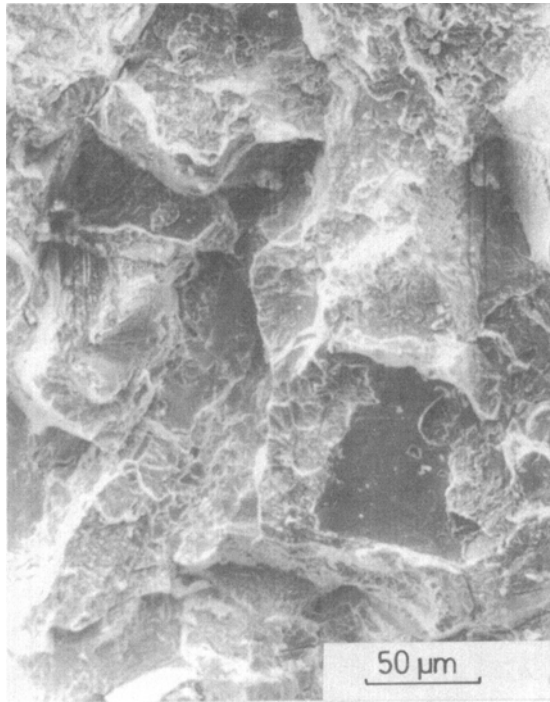
(d)

Fig. 2 Scanning electron images showing fracture surfaces of stock and reprocessed material. (a) Annealed stock material. (b) Higher-magnification view of (a). (c) Remelted and forged material in the annealed condition. (d) Higher-magnification view of (c)

not sufficient to remove the as-cast structure. In contrast, the fracture surfaces in the reprocessed material are representative of a typical ductile fracture, showing dimpled rupture surfaces (Fig. 2c). This indicates that, at least in the case of small-size ingots, 80% reduction was sufficient to remove the as-cast mor-

phology and the segregation effects. The higher-magnification fractograph (Fig. 2d) indicates that the inclusions present within the large dimples were responsible for crack initiation.

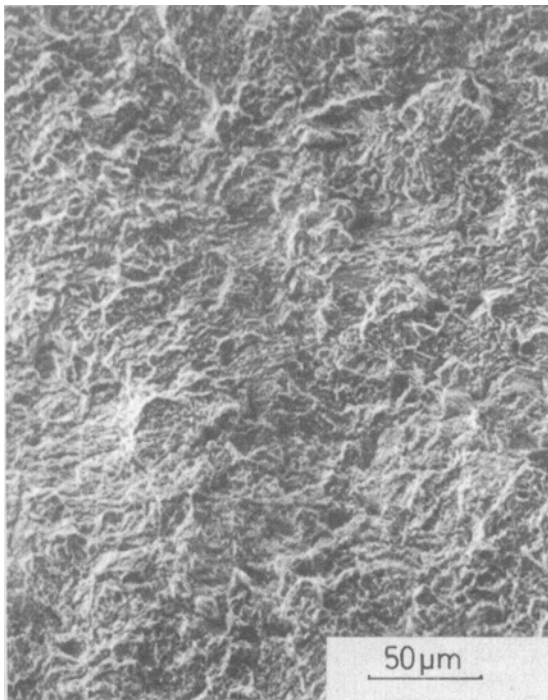
Representative fractographs obtained from the aged specimens are presented in Fig. 3. In the stock material, a mixed-



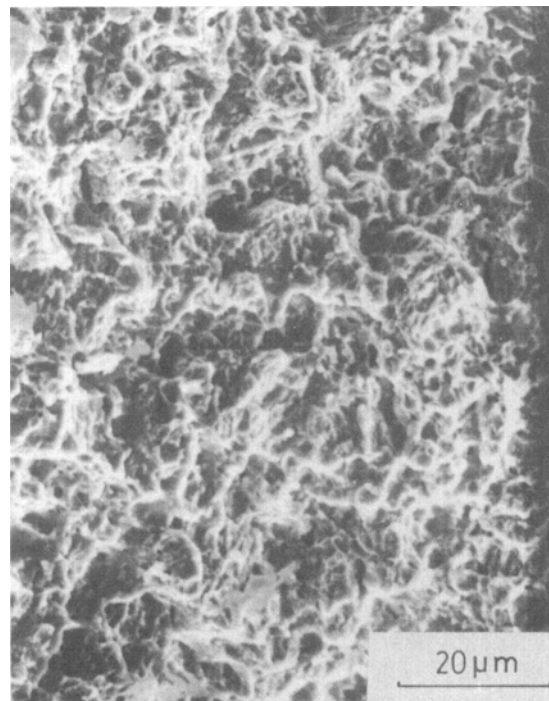
(a)



(b)



(c)



(d)

Fig. 3 Scanning electron images showing fracture surfaces of aged stock and reprocessed material. (a) Stock material. (b) Higher-magnification view of (a). (c) Reprocessed and forged material. (d) Higher-magnification view of (c)

mode type of fracture is visible (Fig. 3a). As in the case of annealed material, both transgranular and intergranular fracture modes are present. In the areas of transgranular fracture, a dendritic type of morphology was again observed (Fig. 3b). In the

reprocessed material, the fracture surfaces exhibited transgranular behavior (Fig. 3c). The high-magnification image (Fig. 3d) reveals dimples, indicating that some plastic deformation occurred before failure.

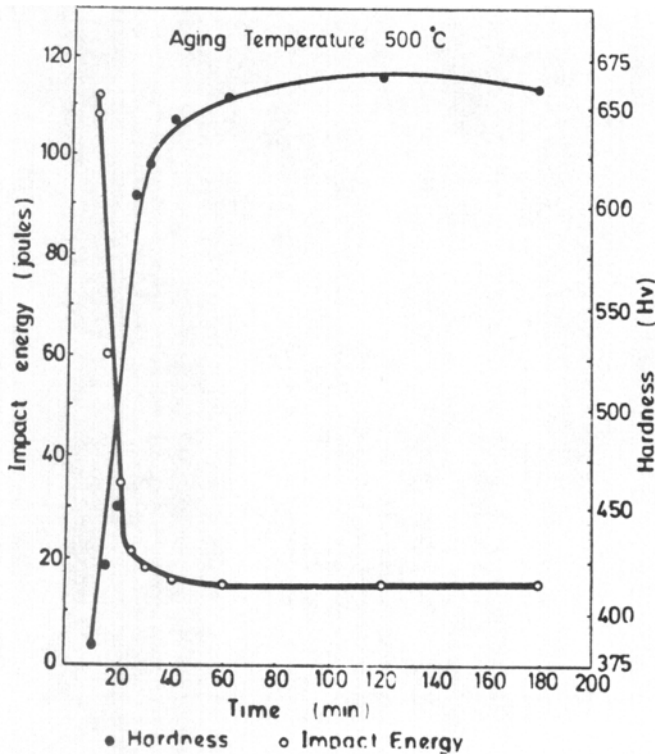


Fig. 4 Variation in hardness and Charpy impact energy as a function of aging time

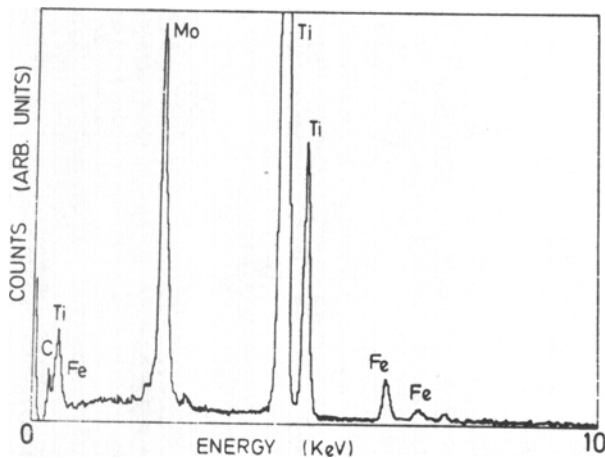


Fig. 5 X-ray spectrum obtained from 100 to 200 nm TiMo(C,N) inclusions

The variations in Charpy fracture toughness values and hardness as a function of aging time were investigated for the case of reprocessed steel. Specimens were aged at 500 °C for the various times indicated in Fig. 4. A sharp decrease in toughness was accompanied by a rapid rise in hardness. The precipitation process proceeded at a very rapid rate, and approximately 90% of the peak hardness was achieved within 25 min. The decrease in toughness has been related to the formation of Ni_3Ti and Fe_2Mo precipitates in the matrix, particu-

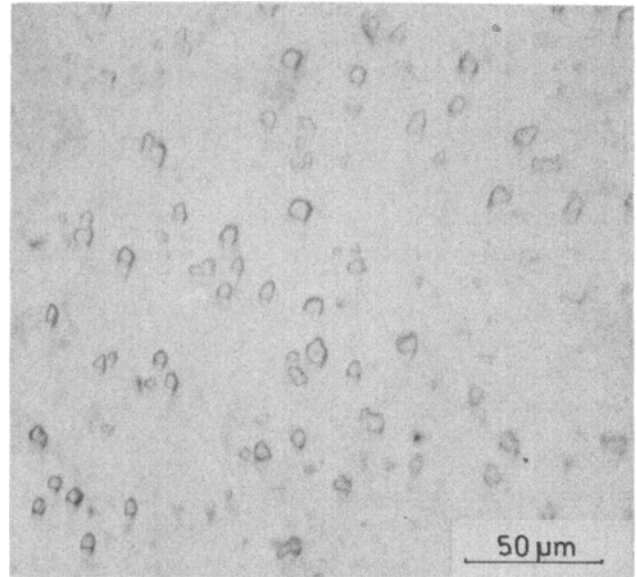


Fig. 6 Optical micrograph depicting TiMo(C,N) inclusions segregated in the top part of an ingot

larly along grain boundaries (Ref 9). An optimum combination of hardness and toughness was obtained after aging for 20 min at 500 °C.

Fine grain size is an important factor regarding the improved toughness values in the case of reprocessed material. However, reduction in grain size alone cannot account for the sharp increase in toughness. As mentioned earlier, the stock material was received in the form of 200 mm diam extruded rod. Examination of fracture surfaces clearly showed that the cast structure was not completely removed in the extrusion process. The presence of as-cast structure was one reason for low fracture toughness—a fact that was confirmed when the stock material was forged along with the reprocessed material. The Charpy fracture toughness values obtained following forging were 60 ± 5 and 6 ± 1 J for the case of annealed and aged specimens, respectively. These values are much higher compared to the as-received extruded material, but are still below the values obtained in the reprocessed material.

The level of inclusions in high-strength materials plays a significant role in determining their overall performance. Examination of the reprocessed and stock material using optical microscopy, SEM, and STEM revealed that the level and size of nonmetallic inclusions were markedly less in the reprocessed material than in the stock material. The stock material exhibited two types of inclusions. First, relatively large (5 to 10 μm), faceted particles were uniformly distributed in the matrix. These inclusions, when analyzed by SEM, produced only a titanium signal (due to the thickness of the detector window, elements below sodium in atomic number could not be analyzed). Most likely, these inclusions were carbonitrides of titanium (Ref 10), which can act as potential crack-initiating sites. The second type of inclusion observed in the stock material was much smaller, ranging from 100 to 200 nm. These inclusions were observed in all the transmission electron microscope (TEM) foils examined, indicating the presence of a very high number

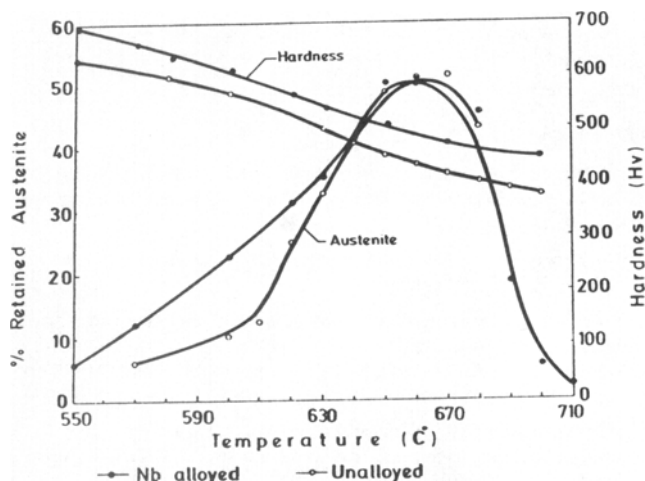


Fig. 7 Variation in hardness and retained austenite content as a function of aging temperature

Table 3 Results of hardness, tensile, and impact testing after addition of 2 wt% Nb

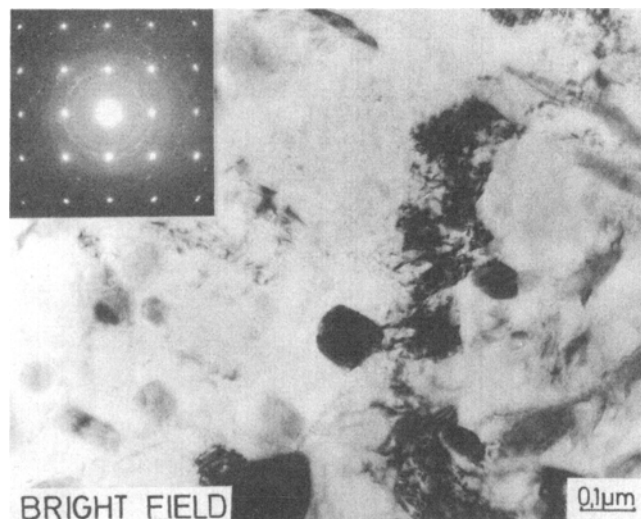
Test	Sample condition(a)	Alloying element (2 wt% Nb)
Hardness, HV	Annealed	358 ± 4
	Aged	740 ± 10
Tensile strength, MPa	Annealed	1435 ± 35
	Aged	2555 ± 70
Charpy V-notch impact values, J	Annealed	33 ± 3
	Aged	10 ± 2

(a) Annealed at 1000 °C for 2 h; aged at 480 °C for 3 h

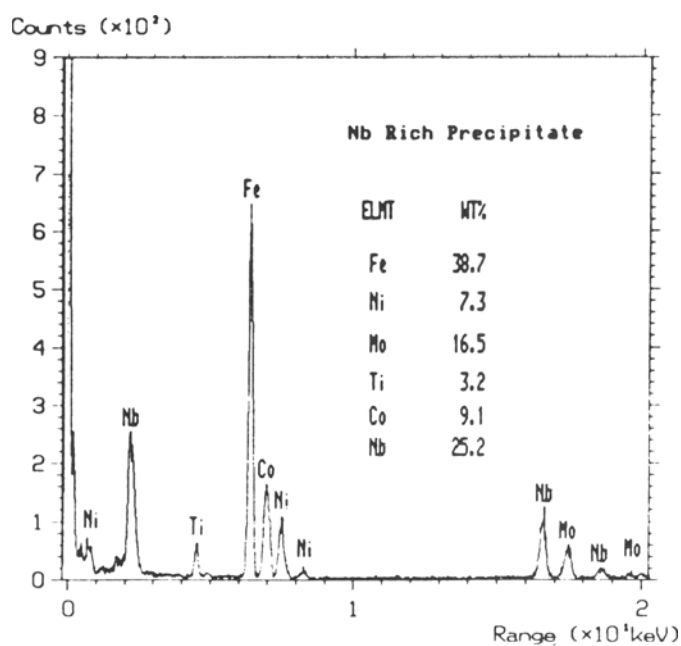
density. The spectrum obtained from these inclusions is presented in Fig. 5. Analysis revealed that the metallic constituents consisted of 80 wt% Ti and 20 wt% Mo. Carbon and nitrogen peaks were also present, but could not be quantified. The analysis clearly showed these inclusions to be carbonitrides of TiMo.

In the reprocessed material, the level of impurities was markedly lower. The inclusions were segregated in the top part of the ingot, which also incorporated the shrinkage cavity and which was removed before forging. An optical micrograph of the segregated inclusions in the hot top of the ingot is shown in Fig. 6. These inclusions were analyzed and found to be carbonitrides of TiMo—similar to the 100 to 200 nm carbonitride inclusions observed in the stock material. The large Ti(C,N)-type inclusions in the stock material were not present in the reprocessed material. Thin foils prepared from the reprocessed material exhibited no evidence of carbonitride inclusions in contrast to the stock material. The overall reduction in inclusion level, along with the refined microstructure, likely resulted in the improved properties of the reprocessed material.

During reprocessing some of the titanium was lost, which in turn affected the maximum hardness achieved after aging. To compensate for this loss, elemental titanium was added during remelting. Hardness greater than 740 HV was obtained after forging and subsequent aging at 480 °C for 3 h. However, the Charpy impact value deteriorated substantially and was on the



(a)



(b)

Fig. 8 (a) TEM micrograph of the niobium-alloyed maraging steel. (b) X-ray spectrum obtained from the niobium-rich precipitate

order of 4 ± 1 J. It was determined that the low impact strength was due to the presence of nonmetallic inclusions, such as titanium oxide and Ti(C,N), which probably formed during remelting. The elemental titanium added was in the form of 0.25 mm diam granules, and it is quite likely that the large surface area encouraged the formation of highly detrimental oxides. It was subsequently observed that addition of titanium in larger lumps (several millimeters in size) improved the toughness characteristics of reprocessed material.

Niobium is known to form intermetallic compounds with most of the elements present in maraging steel. Addition of 2 wt% Nb resulted in improved hardness without compromising

toughness (Table 3). The maximum hardness and the corresponding Charpy impact values obtained in the specimens aged at 480 °C for 3 h were 740 ± 10 HV and 10 ± 2 J, respectively. For this steel it was observed that annealing at 1000 °C for 2 h produced optimum results following aging. Addition of niobium improved the overall hardness as a function of aging temperature and also influenced the amount of reverted austenite obtained following aging. Figure 7 shows the hardness values as well as reverted austenite content, plotted as a function of aging temperature in niobium-alloyed and unalloyed steel. The specimens were aged for 1 h at the indicated temperatures. Figure 7 clearly demonstrates that niobium acts as an austenite stabilizer. Examination of the aged specimens by TEM revealed that, in addition to the presence of Ni_3Ti and Ni_2Mo precipitates, niobium-rich precipitates, about 100 nm in diameter, were uniformly distributed in the martensite matrix (Fig. 8a). The EDX spectrum obtained from these precipitates is shown in Fig. 8(b). At present, the electron diffraction patterns from these precipitates do not conform to any known phases in the system. Work is currently underway to identify these precipitates.

4. Summary

Maraging steel scrap can be successfully utilized by remelting in a vacuum induction melting and casting furnace and then hot forging. Except for some loss of titanium, the composition of the remelted steel is well within prescribed limits. Alloying with 2 wt% Nb enhances hardness without sacrificing toughness.

Acknowledgments

The authors would like to thank Mr. Mehrab Gul for his help in the melting shop. Thanks are also due to Mr. Tahir M. Khan

and Mr. Liaqat Ali for their help in photography and drafting, respectively.

References

1. R.F. Decker, J.T. Eash, and A.J. Goldman, 18% Ni Maraging Steels, *Source Book on Maraging Steel*, American Society for Metals, 1979, p 1-19
2. *Maraging Steel—Recent Developments and Applications*, K. Wilson, Ed., TMS, 1988
3. B.Z. Weiss, Maraging Steels—Structures, Properties and Applications, *Proc. Int. Conf. on Recent Developments in Specialty Steels and Hard Materials*, N.R. Comins and J.B. Clark, Ed., Pergamon Press, 1983, p 35-54
4. V.K. Vasudevan, S.J. Kim, and C.M. Wayman, Precipitation Reactions and Strengthening Behavior in 18 wt.% Ni Maraging Steels, *Metall. Trans.*, Vol 21A, 1990, p 2655-2668
5. D.T. Peters, A Study of Austenite Reversion during Aging of Maraging Steels, *Trans. ASM*, Vol 61, 1968, p 304-316
6. H. Hosomi, T. Nakamura, and H. Nakamura, Austenite Reverse Transformation in 18% Ni Maraging Steel during Heating, *Proc. Int. Conf. on Martensite Transformation*, Japan Institute of Metals, 1986, p 566-571
7. M. Ahmed, S.K. Hasnain, F.H. Hashmi, and A.Q. Khan, The Magnetic Properties of Maraging Steel in Relation to Structural Phase Transformations, *Proc. MRS Int. Meet. on Advanced Material* (Tokyo), Vol 11, 1988
8. M. Ahmed, I. Nasim, I. Salam, F.H. Hashmi, and A.Q. Khan, Re-processing and Additional Alloying of 18Ni-350 Maraging Steel, *Proc. 2nd Int. Symp. on Advanced Materials*, A. ul Haq, N. Ahmad, and A.Q. Khan, Ed., 1991, p 170-180
9. I.L. Cheng and G. Thomas, Structure and Properties of Fe-Ni-Co-Ti Maraging Steel, *Trans. ASM*, Vol 61, 1968, p 14-25
10. A.J. Birkle, D.S. Dabkowski, J.P. Paulina, and L.F. Poater, A Metallographic Investigation of the Factors Affecting the Notch Toughness of Maraging Steels, *Trans. ASM*, Vol 58, 1965, p 123-139